Alterations in cellular metabolism triggered by *URA7* or *GLN3* inactivation cause imbalanced dNTP pools and increased mutagenesis

Tobias T. Schmidt[a], Gloria Reyes[a], Kerstin Gries[a], Cemile Ümran Ceylan[a], Sushma Sharma[b], Matthias Meurer[a,c], Michael Knop[a,c], Andrei Chabes[b,d], and Hans Hombauer[a,1]

[a]German Cancer Research Center, 69120 Heidelberg, Germany; [b]Department of Medical Biochemistry and Biophysics, Umeå University, SE-901 87 Umea, Sweden; [c]Zentrum für Molekulare Biologie der Universität Heidelberg, 69120 Heidelberg, Germany; and [d]Laboratory for Molecular Infection Medicine Sweden, Umeå University, SE-901 87 Umea, Sweden

Edited by Richard D. Kolodner, Ludwig Institute for Cancer Research, La Jolla, CA, and approved March 28, 2017 (received for review December 15, 2016)

Eukaryotic DNA replication fidelity relies on the concerted action of DNA polymerase nucleotide selectivity, proofreading activity, and DNA mismatch repair (MMR). Nucleotide selectivity and proofreading are affected by the balance and concentration of deoxyribonucleotide (dNTP) pools, which are strictly regulated by ribonucleotide reductase (RNR). Mutations preventing DNA polymerase proofreading activity or MMR function cause mutator phenotypes and consequently increased cancer susceptibility. To identify genes not previously linked to high-fidelity DNA replication, we conducted a genome-wide screen in *Saccharomyces cerevisiae* using DNA polymerase active-site mutants as a "sensitized mutator background." Among the genes identified in our screen, three metabolism-related genes (*GLN3*, *URA7*, and *SHM2*) have not been previously associated to the suppression of mutations. Loss of either the transcription factor Gln3 or inactivation of the CTP synthetase Ura7 both resulted in the activation of the DNA damage response and imbalanced dNTP pools. Importantly, these dNTP imbalances are strongly mutagenic in genetic backgrounds where DNA polymerase function or MMR activity is partially compromised. Previous reports have shown that dNTP pool imbalances can be caused by mutations altering the allosteric regulation of enzymes involved in dNTP biosynthesis (e.g., RNR or dCMP deaminase). Here, we provide evidence that mutations affecting genes involved in RNR substrate production can cause dNTP imbalances, which cannot be compensated by RNR or other enzymatic activities. Moreover, Gln3 inactivation links nutrient deprivation to increased mutagenesis. Our results suggest that similar genetic interactions could drive mutator phenotypes in cancer cells.

DNA replication fidelity | mismatch repair | CTP biosynthesis | DNA polymerases | dNTP pool imbalance

The fidelity of DNA replication is strongly influenced by three processes (1–3): (*i*) nucleotide selectivity, wherein replicative DNA polymerases select the correct dNTP to be incorporated; (*ii*) DNA polymerase proofreading activity, which excises wrongly incorporated nucleotides by using the DNA polymerase 3′-to-5′ exonuclease activity; and (*iii*) mismatch repair (MMR) (4, 5), a DNA replication-coupled repair mechanism (6, 7), which corrects errors that escaped proofreading. Furthermore, the balance and overall concentration of dNTPs not only affect nucleotide selection but also influence DNA polymerase proofreading activity (8). A central player in the biosynthesis of dNTPs is the ribonucleotide reductase (RNR) holoenzyme, which catalyzes the reduction of NDPs to dNDPs (9, 10). In *Saccharomyces cerevisiae*, RNR is composed of two identical Rnr1 large subunits that associate with two smaller subunits represented by Rnr2 and Rnr4 (11, 12). In addition, a second large subunit has been identified (Rnr3), which is induced upon DNA damage and when overexpressed can rescue the *rnr1* lethal phenotype (13).

The interplay between nucleotide selectivity, DNA polymerase proofreading activity, and MMR guarantees the high accuracy of DNA replication, resulting in less than one mutation per genome duplication in *S. cerevisiae* (14–16). Perturbations in any of these processes are linked to increased mutation rates and, in higher eukaryotes, to increased cancer susceptibility. Accordingly, mutations inactivating DNA polymerase proofreading function or MMR genes are associated with familial colorectal/ovarian cancer (17, 18) and Lynch syndrome (19), respectively.

Eukaryotic DNA synthesis is accomplished by three essential DNA polymerases: Polα, Polε, and Polδ (called in *S. cerevisiae* Pol1, Pol2, and Pol3, respectively). Polα initiates DNA synthesis at replication origins and at every Okazaki fragment, albeit with low processivity and lack of proofreading activity. Subsequently, the synthesis is taken over by one of the two high-fidelity DNA polymerases, Polε or Polδ. Polε replicates the leading strand, whereas Polδ synthesizes the lagging strand. This "division of labor during eukaryotic DNA replication" model (20) was initially proposed based on the characterization of *S. cerevisiae* strains carrying active-site mutations in DNA polymerases (e.g., *pol2-M644G* and *pol3-L612M*), which confer a weak mutator phenotype with a characteristic mutator signature, without compromising DNA polymerase proofreading activity (21, 22).

Given the intrinsic mechanistic differences between leading- and lagging-strand DNA synthesis, it has been proposed that the two strands may also differ in terms of repair efficiencies. Supporting this idea, reports have shown that errors made in the lagging strand (especially those generated by Pol1) are more efficiently repaired by MMR than errors made in the leading strand (23, 24). In addition, inactivation of yeast Exo1, a 5′–3′ exonuclease that is involved in

Significance

The duplication of the genetic information (DNA) requires high accuracy to prevent potentially deleterious genetic alterations (mutations). The fidelity of this reaction depends on DNA polymerase selectivity and proofreading functions, postreplicative mismatch repair (MMR), and the abundance of dNTPs, the building blocks of DNA. Here, in a genome-wide screen in budding yeast, we uncovered a group of genes required for high-fidelity DNA replication. When these genes are absent, cells are prone to incorporate incorrect nucleotides, and consequently they heavily rely on DNA polymerase functions and MMR to prevent severe hypermutability. These findings suggest that similar genetic interactions could play a role in human cancer, where inactivation of these genes might act as "minidrivers" that facilitate tumor evolution.

Author contributions: T.T.S., G.R., and H.H. designed research; T.T.S., G.R., K.G., C.Ü.C., S.S., and H.H. performed research; M.M. and M.K. contributed new reagents/analytic tools; T.T.S., G.R., K.G., C.Ü.C., S.S., A.C., and H.H. analyzed data; and T.T.S., G.R., and H.H. wrote the paper.

The authors declare no conflict of interest.

This article is a PNAS Direct Submission.

See Commentary on page 5561.

[1]To whom correspondence should be addressed. Email: h.hombauer@dkfz.de.

This article contains supporting information online at www.pnas.org/lookup/suppl/doi:10.1073/pnas.1618714114/-/DCSupplemental.

MMR (25), increased the mutation rates to a greater extent when combined with mutant variants of the lagging-strand polymerases (*pol1-L868M* or *pol3-L612M*) than when combined with a mutator variant of the leading-strand polymerase (*pol2-M644G*) (26, 27). This suggests that lagging-strand MMR might be more dependent on Exo1 function than leading-strand MMR.

In this study, we conducted a genome-wide screen in *S. cerevisiae* in which we used three active-site DNA polymerase mutants to identify genes that prevent the accumulation of mutations. We uncovered a group of genes that are important for ensuring the fidelity of DNA replication, especially when DNA polymerase or MMR function is compromised. We discovered that inactivation of either the transcription factor Gln3 or the CTP synthetase Ura7 results in reduced dCTP concentrations and DNA damage checkpoint activation, with concomitant up-regulation of the other three dNTPs. Moreover, we showed that glutamine supplementation suppresses mutagenesis in *gln3Δ* mutants, providing evidence for a link between nutrient deprivation and mutator phenotypes. Mutation spectra analysis in *ura7Δ* and *gln3Δ* mutants revealed a mutation signature dominated by C-to-T transitions, which is likely driven by an increased dTTP:dCTP ratio observed in the absence of either of these two genes. Overall, we have found an additional requirement for dNTP pool homeostasis, defined by genes that affect the production of one of the substrates used by RNR. We demonstrated that inactivation of these genes creates a dNTP pool imbalance with high mutagenic potential that, in combination with genetic alterations affecting DNA polymerase nucleotide selectivity, proofreading activity, or MMR, causes a strong mutator phenotype.

Results

A Genome-Wide Screen Uncovers Genes Required for DNA Replication Fidelity. Numerous studies in *S. cerevisiae* have shown that DNA polymerase mutations, in combination with MMR mutant alleles, lead to synergistic mutator interactions (28–31). We rationalized that, by using DNA polymerase mutants as a "sensitized mutator background," we may identify previously unrecognized genes that contribute to DNA replication fidelity. For this purpose, we performed a genome-wide screen where we crossed a nonessential yeast deletion collection (~4,800 strains) with either a wild-type (WT) strain, or one of three DNA polymerase active-site mutants (*pol1-L868M*, *pol2-M644G*, and *pol3-L612M*), followed by mutator phenotype evaluation. These active-site mutations cause a mild mutator phenotype, allowing us to screen for mutational enhancers. We engineered a modified version of the synthetic genetic array (SGA) protocol (32) to select for haploid cells that simultaneously carry the DNA polymerase mutation, a nonessential gene deletion, and two mutator reporters, one frameshift reporter (*lys2-10A*), and one forward inactivation reporter (*CAN1*) (Fig. 1*A*). To increase the robustness of the screen, we crossed in quadruplicate the deletion collection with the four query strains. Due to the large number of strains, we aimed to screen for mutator phenotypes (~4,800 strains × 4 queries × 4 ~ 77,000 strains), we set up a "semi–high-throughput" method in 96-well format, in which each plate contained up to 24 different genotypes. Cells were spotted in yeast extract–peptone–dextrose (YPD) agar plates, grown, and replica plated on reporter plates lacking lysine (*lys2-10A* frameshift assay) or containing canavanine (*CAN1* inactivation assay). After 4 d of incubation, plates were scored for increased number of colonies, which is indicative of potential mutator phenotypes. Fig. 1*B* illustrates two single mutants showing increased mutator phenotypes. The *msh6Δ* mutant, which shows a partial MMR deficiency (33), resulted in frameshifts (lysine− plate) and increased *CAN1* inactivating mutations (+canavanine plate). Moreover, the *ubc13Δ* mutant that is defective in error-free postreplication repair (34) caused increased *CAN1* inactivation but not frameshifts.

A previous screen done in *S. cerevisiae* identified 33 genes with different roles in DNA replication and repair (among others) that, when inactivated, caused elevated mutator phenotypes (35). In contrast, we concentrated our work on deletion mutants that confer strong mutator phenotypes in the presence of DNA polymerase mutant alleles.

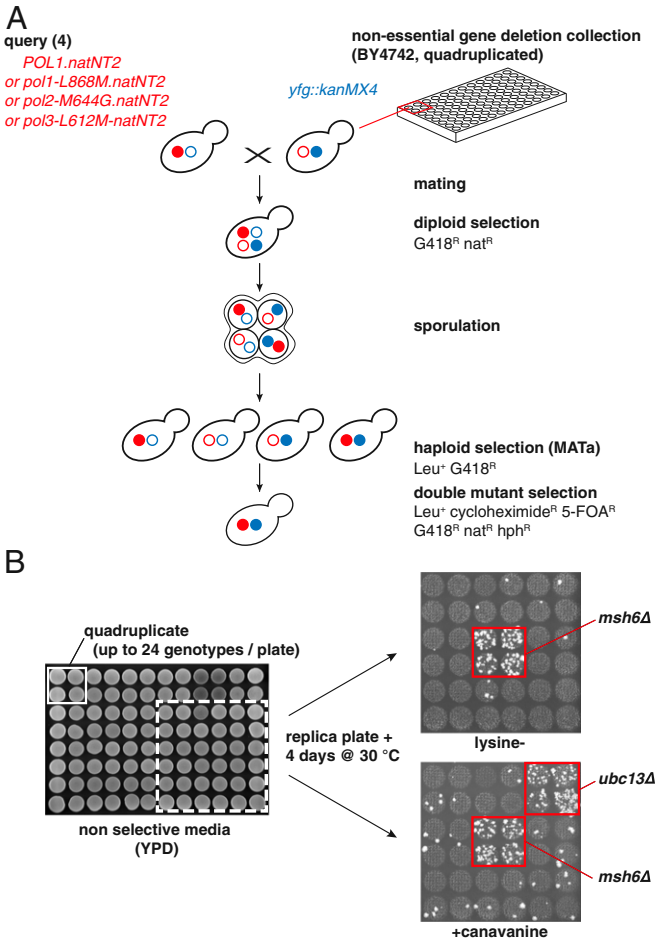

Fig. 1. Genome-wide screen identifies genes that affect DNA replication fidelity in *S. cerevisiae*. (*A*) Strategy used to cross the nonessential gene deletion collection with active-site DNA polymerase mutants. (*B*) To screen for mutator phenotypes in 96-well format, strains were spotted on YPD, grown, and replica plated on mutator reporter plates. Increased number of colonies is indicative of a potential mutator phenotype. On the right side (zoom-in), *msh6Δ* results in increased frameshifts (lysine−) and *CAN1* mutations (+canavanine), whereas *ubc13Δ* increases *CAN1* mutations, exclusively.

Qualitative mutator analysis of the double mutants uncovered a group of genes (*GLN3*, *SHM2*, *URA7*, *RRM3*, and *EXO1*) that, when inactivated in specific DNA polymerase mutant backgrounds, resulted in strong mutator phenotypes, evidenced by an increased abundance of canavanine-resistant (Can^R) colonies (three representative examples are shown in Fig. S1). None of these double mutants (with the exception of *exo1Δ* combinations) showed an increased mutator phenotype in the *lys2-10A* frameshift assay, suggesting that the Can^R mutator phenotypes are likely a consequence of base substitutions (Fig. S1).

Besides *EXO1*, all other identified genes have not been previously linked to an increased mutator phenotype. Intriguingly, most of these gene deletions (*GLN3*, *SHM2*, *URA7*, and *EXO1*) caused strong mutator phenotypes exclusively in the lagging-strand DNA polymerase mutant backgrounds (*pol1-L868M* and *pol3-L612M*). Moreover, *gln3Δ*, *shm2Δ*, *ura7Δ*, and *rrm3Δ* did not cause a mutator phenotype in the presence of WT DNA polymerases, suggesting that DNA polymerases buffer against mutations in the absence of these genes.

Gln3, Shm2, and Ura7 regulate genes or metabolic reactions that are linked to the synthesis of purines and pyrimidines. Specifically, Ura7 converts UTP into CTP, which is then used as substrate for the production of dCTP and dTTP (36, 37); Gln3 is

a transcription factor that controls nitrogen metabolism (38, 39); and last, Shm2 is a serine hydroxymethyltransferase part of the one-carbon (C1) metabolism (40, 41). On the other hand, Exo1 and the helicase Rrm3 belong to the group of proteins implicated in DNA repair and genome stability (42–45).

To validate our initial findings, we first generated de novo single and double mutants and determined their mutation rates by fluctuation analysis (Table 1). In agreement with initial findings, *gln3Δ*, *shm2Δ*, *ura7Δ*, and *rrm3Δ* single mutants showed mutation rates that were indistinguishable from WT strain. Notably, we found that inactivation of *GLN3*, *SHM2*, *URA7*, or *EXO1* resulted in a synergistic increase in the mutation rates when combined with mutator variants of the lagging-strand DNA polymerases (*pol1-L868M* or *pol3-L612M*), but not when combined with a leading-strand polymerase mutant (*pol2-M644G*) (Table 1). The double-mutants *pol1-L868M ura7Δ* and *pol1-L868M gln3Δ* showed the highest *CAN1* mutation rates, which were 323- and 293-fold higher than WT (or 65- and 59-fold higher than *pol1-L868M* mutant), respectively. A similar synergistic increase was observed in *ura7Δ* or *gln3Δ* mutants in combination with *pol1-L868M* or *pol3-L612M* (but not with *pol2-M644G*) in an alternative forward mutation assay based on the inactivation of the *URA3* gene (Table S1). Thus, these results further demonstrate that these double-mutant combinations result in an overall increased mutator phenotype. To test whether the mutator phenotype observed in *pol3-L612M ura7Δ* (or *pol3-L612M gln3Δ*) double mutant depends on error-prone translesion synthesis (TLS) DNA polymerases (Polζ, Polη, or Rev1) (46), we measured the mutation rates in *pol3-L612M gln3Δ* and *pol3-L612M ura7Δ* strains lacking Polζ (*rev3Δ*), Polη (*rad30Δ*), or Rev1 (*rev1Δ*) polymerases. We found that, in the absence of TLS polymerases, the mutation rates were not reduced (Table S2); therefore, these genes are not responsible for the mutator phenotype.

Unlike *gln3Δ*, *ura7Δ*, *exo1Δ*, and *shm2Δ* mutants that predominantly interacted with *pol1-L868M* and *pol3-L612M*, the *rrm3Δ* mutant mainly interacted with *pol2-M644G* and *pol3-L612M*, resulting in mutation rates 40-fold and 50-fold higher than WT, respectively (or threefold and fourfold higher than the polymerase mutants) (Table 1).

Inactivation of Gln3 or Ura7 Results in a Mutagenic Potential That Is Counteracted by DNA Polymerase Proofreading Function and MMR Activity. Because DNA replication fidelity depends not only on nucleotide selectivity but also on DNA polymerase proofreading activity and MMR function, we tested the consequences of the loss of Gln3, Shm2, Ura7, and Rrm3 in three genetic backgrounds with partially compromised MMR function (*exo1Δ*, *msh3Δ*, and *msh6Δ*) (33, 47), complete lack of MMR (*msh2Δ*) (33), or in the absence of Polε proofreading activity (*pol2-04* mutant allele) (48). Inactivation of *GLN3* or *URA7* in all tested backgrounds, with the exception of *msh3Δ*, resulted in strong synergies in the *CAN1* inactivation assay (Table 2 and Table S3). For example, *exo1Δ gln3Δ* resulted in a 15-fold higher mutation rate than *exo1Δ*, and *msh6Δ ura7Δ* resulted in 40-fold increase over *msh6Δ* strain. Inactivation of *RRM3* or *SHM2* in an *msh6Δ* background caused a smaller increase in *CAN1* inactivation (5.1- and 2.2-fold over *msh6Δ* strain, respectively) and had no effect in the *CAN1* inactivation rate in an *exo1Δ* background.

Exo1Δ gln3Δ and *exo1Δ ura7Δ* double mutants also showed increased levels of frameshift mutations (Table S3). We confirmed these frameshifts by sequencing 50 independent *hom3-10* revertants (Thr^+) from *exo1Δ gln3Δ* and *exo1Δ ura7Δ* double mutants. We found that all Thr^+ revertants contained the same single-nucleotide deletion (−1 T) in a run of 7 Ts (starting at nucleotide 646), a hotspot for frameshift mutations previously identified in MMR-deficient mutants (33).

Mutational analysis in *msh2Δ shm2Δ*, *msh2Δ gln3Δ*, *msh2Δ ura7Δ*, and *msh2Δ rrm3Δ* double mutants revealed 1.4-, 2.4-, 6.6-, and 3.1-fold increase in the *CAN1* inactivation rate (compared with *msh2Δ* strain), respectively, without a significant impact on frameshift mutations (Table S3). With the exception of *msh2Δ shm2Δ* mutant, all other double mutants showed *CAN1* inactivation rates significantly higher than *msh2Δ* strain (according to 95% confidence intervals).

Inactivation of *MSH3* in *gln3Δ*, *shm2Δ*, *ura7Δ*, or *rrm3Δ* mutant backgrounds revealed no major changes in the mutation rates, with the exception of *msh3Δ rrm3Δ*, which showed a small increase in all three assays (Table S3). These observations are in agreement with the predominant role of Msh6 over Msh3 in MMR, specifically in the repair of base substitutions (33).

Double-mutant combinations of *gln3Δ* or *ura7Δ* with *pol2-04* revealed synergistic increases in the *CAN1* mutation rates (Table 2). For example, *pol2-04 gln3Δ* and *pol2-04 ura7Δ* double mutants resulted in 26- and 59-fold increase over *pol2-04*, respectively. Together, these findings indicate that loss of Gln3 or Ura7 predisposes to base substitutions that are prevented by DNA polymerases or corrected by MMR. On the other hand, inactivation of Shm2 or Rrm3 in *msh6Δ*, *msh2Δ*, or *pol2-04* mutant backgrounds resulted in a less pronounced increase in the mutation rates (Table 2 and Table S3). These results may reflect a smaller contribution of Shm2 and Rrm3 in DNA replication fidelity, compared with either Ura7 or Gln3.

Despite several attempts, we could not obtain a *ura7Δ* mutant in a Polδ proofreading-defective background (*pol3-01*) (28) by yeast matings. This observation suggested that the *pol3-01 ura7Δ* double-mutant combination might result in synthetic lethality or severe growth defect. Similar genetic interactions have been previously described for *pol3-01* in combination with mutations that abolish MMR function (e.g., *msh2Δ* combined with *pol3-01*) (29), supporting a model in which the extreme mutator phenotype results in "error-induced extinction" (28, 31). Indeed, plasmid-shuffling experiments in a haploid *pol3Δ ura7Δ* strain complemented by a *pol3-01* plasmid ("*ura7Δ* + *pol3-01*") revealed a strong growth defect (Fig. 2*A*), which was less severe in a diploid homozygous *pol3Δ ura7Δ* strain complemented with the same plasmid (Fig. 2*B*). This observation is in agreement with the ∼10-fold higher error extinction threshold that a diploid strain (compared with haploids) can tolerate (49). Moreover, even a diploid *ura7Δ* + *pol3-01* strain showed reduced proliferation rates compared with isogenic strains transformed with WT *POL3* plasmid (Fig. 2*C*). As *ura7Δ* + *pol3-01* haploid mutants showed severe growth defects, we determined

Table 1. Mutation rate analysis of the mutants identified in this screen in combination with DNA polymerase active-site mutant alleles

	Mutation rate (fold increase)* Can^R			
Relevant genotype	WT	*pol1-L868M*	*pol2-M644G*	*pol3-L612M*
WT	7.2 [5.7–9.0] × 10^{-8} (1)	3.9 [3.3–4.9] × 10^{-7} (5)	8.4 [7.3–10.6] × 10^{-7} (12)	9.3 [7.7–11.6] × 10^{-7} (13)
exo1Δ	7.4 [6.3–9.8] × 10^{-7} (10)	5.7 [3.1–8.1] × 10^{-6} (80)	1.9 [1.1–2.9] × 10^{-6} (26)	6.5 [3.6–10.8] × 10^{-6} (91)
gln3Δ	1.0 [0.8–1.2] × 10^{-7} (1)	2.1 [1.4–4.5] × 10^{-5} (293)	3.3 [2.6–6.0] × 10^{-7} (5)	9.1 [7.3–18.2] × 10^{-6} (127)
shm2Δ	1.2 [1.1–1.7] × 10^{-7} (2)	1.7 [1.0–2.0] × 10^{-6} (23)	5.5 [3.9–7.3] × 10^{-7} (8)	3.6 [2.1–4.7] × 10^{-6} (50)
ura7Δ	1.0 [0.9–1.5] × 10^{-7} (1)	2.3 [1.3–4.1] × 10^{-5} (323)	1.1 [0.7–1.5] × 10^{-6} (15)	1.6 [1.1–2.6] × 10^{-5} (218)
rrm3Δ	1.1 [0.8–1.5] × 10^{-7} (2)	3.5 [2.1–4.4] × 10^{-7} (5)	2.8 [1.9–4.8] × 10^{-6} (40)	3.6 [2.6–6.0] × 10^{-6} (50)

*Median rates of inactivation of *CAN1* gene (Can^R) with 95% confidence interval in square brackets and fold increase relative to the WT in parentheses.

Table 2. Mutation rate analysis of the mutants identified in this screen in combination with alleles causing reduced DNA replication fidelity

Relevant genotype	Mutation rate (fold increase)* Can^R			
	WT	*exo1Δ*	*msh6Δ*	*pol2-04*
WT	7.2 [5.7–9.0] × 10^{-8} (1)	7.4 [6.3–9.8] × 10^{-7} (10)	9.6 [7.8–11.7] × 10^{-7} (13)	6.2 [4.3–7.6] × 10^{-7} (6)
gln3Δ	1.0 [0.8–1.2] × 10^{-7} (1)	1.1 [0.8–1.4] × 10^{-5} (146)	2.4 [1.7–3.4] × 10^{-5} (334)	1.1 [0.9–1.6] × 10^{-5} (154)
shm2Δ	1.2 [0.8–2.8] × 10^{-7} (2)	8.4 [7.1–10.5] × 10^{-7} (12)	2.1 [1.3–2.6] × 10^{-6} (30)	1.5 [1.1–2.3] × 10^{-6} (22)
ura7Δ	1.0 [0.9–1.5] × 10^{-7} (1)	1.9 [0.8–2.4] × 10^{-5} (261)	3.8 [3.2–8.5] × 10^{-5} (524)	2.5 [1.8–5.2] × 10^{-5} (354)
rrm3Δ	1.1 [0.8–1.5] × 10^{-7} (2)	6.3 [4.3–7.6] × 10^{-7} (9)	4.9 [3.6–7.3] × 10^{-6} (68)	1.4 [0.9–1.8] × 10^{-6} (19)

*Median rates of inactivation of *CAN1* gene (Can^R) with 95% confidence interval in square brackets and fold increase relative to the WT in parentheses.

CAN1 mutation rates in *ura7Δ* + *pol3-01* diploid strains hemizygous for the *CAN1* locus (*CAN1/can1Δ*) (Fig. 2*D*). Remarkably, we found that *ura7Δ* + *pol3-01* diploid strain has a mutation rate of 1.6×10^{-3} (6.482-fold higher than a WT diploid strain). This mutation rate is at the error extinction threshold (1×10^{-3} mutations per cell division) reported for haploids (49) but is below the one for diploids (1×10^{-2} mutations per cell division), arguing that the severe growth defect observed in haploids is a consequence of error-induced extinction. These findings demonstrate that Ura7 inactivation leads to an extreme mutator phenotype, which in the absence of Pol3 proofreading activity is almost incompatible with cell viability.

Loss of Gln3 or Ura7 Causes Activation of the DNA Damage Response. Three of the mutants identified here (*gln3Δ*, *ura7Δ*, and *rrm3Δ*) were previously shown to have an extended S-phase (50). Because a prolonged S-phase could indicate DNA damage or replication stress, we investigated whether *gln3Δ* or *ura7Δ* mutants show activation of the DNA damage response (DDR) (Fig. 3*A*), similar as described for *rrm3Δ* mutant (51). DNA damage or replication stress triggers phosphorylation of checkpoint kinase Rad53 (52, 53), which in turns activates checkpoint kinase Dun1. Dun1 phosphorylation results in the inhibition of three repressors of RNR: Sml1, which binds and inhibits RNR1 (54, 55); Crt1, which acts as a transcriptional repressor of RNR2–4 (12, 13, 56); and Dif1, which prevents RNR cytoplasmic holoenzyme assembly by sequestering Rnr2–Rnr4 into the nucleus (57, 58). Thus, phosphorylation of Dun1 releases the negative regulation on RNR, promoting high expression levels of RNR subunits (RNR1–4) and RNR holoenzyme assembly, consequently resulting in increased dNTP production (59) (Fig. 3*A*).

Analysis of whole-cell lysates in *ura7Δ* and *gln3Δ* mutants by Western blotting revealed that both deletions cause constitutive DDR activation, characterized by Rad53 phosphorylation (as evidenced by a retarded Rad53 electrophoretic mobility) and elevated Rnr2 and Rnr4 levels (and increased Rnr3 levels in *ura7Δ* mutant) (Fig. 3*B*). Loss of Shm2 did not affect Rad53 phosphorylation or RNRs levels with the exception of Rnr4, which was slightly elevated. Accordingly, mutants with constitutive activation of DDR, like *pol2-M644G* (60) or as shown here *gln3Δ* and *ura7Δ* deletion mutants, all presented an accumulation of cells in S-phase (Fig. 3*C*). Unlike *pol2-M644G*, other active-site DNA polymerase mutants (*pol1-L868M* and *pol3-L612M*) did not cause activation of DDR (Fig. 3 *B* and *C*).

Previous reports have shown that mutator phenotypes observed in strains carrying DNA polymerase mutations preventing proofreading (*pol2-04* or *pol3-01*) (31, 60, 61) or altering nucleotide selectivity function (*pol3-L612M* or *pol3-R696W*) (49, 62) can be suppressed by deletion of *DUN1*, which leads to reduced dNTP pools. To test whether the strong mutator phenotypes identified here can be modulated by dNTP levels, we introduced the *dun1Δ* mutation in several double mutants. Notably, deletion of *DUN1* almost completely suppressed the *CAN1* mutator phenotype in *pol1-L868M gln3Δ* from 293-fold to 4-fold over the WT rate (Fig. 3*D*). Similar results were obtained when the *dun1Δ* mutation was introduced in *pol3-L612M ura7Δ*, *pol2-04 gln3Δ*, and *pol3-L612M gln3Δ* double mutants (Fig. 3*D* and Table S3). Interestingly, we found that deletion of *DUN1* in

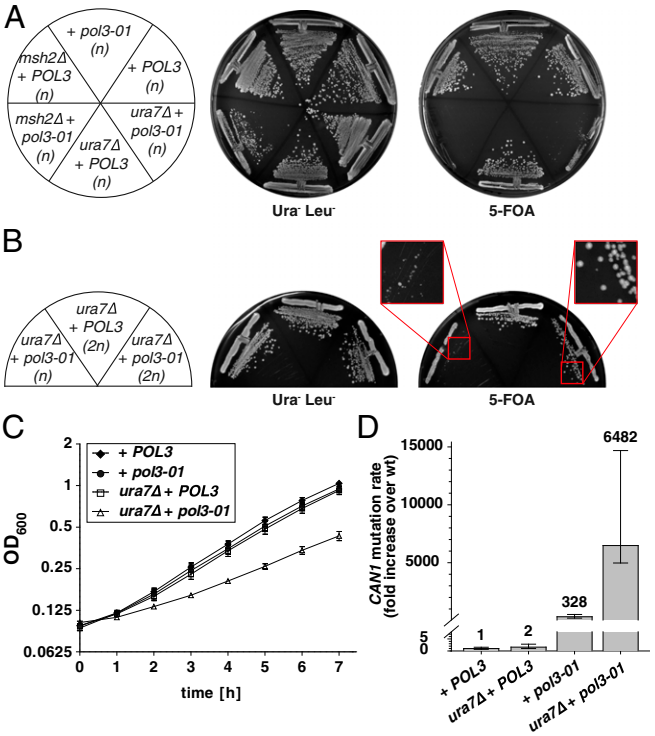

Fig. 2. Inactivation of *URA7* in Pol3 proofreading-defective background (*pol3-01*) results in severe growth defects and synergistic increases in mutation rates. (*A*) Plasmid shuffling strains *pol3Δ*, *pol3Δ ura7Δ*, and *pol3Δ msh2Δ* [all haploids (*n*) complemented with a WT *POL3-URA3* plasmid] were transformed with either WT *POL3* or *pol3-01 LEU2*-plasmids. Transformants were grown on Ura^- Leu^- SD plates or 5-FOA–containing plates to select against WT *POL3-URA3* plasmid. Double-mutant combination *msh2Δ* + *pol3-01* serves as positive control for a synthetic lethal interaction. (*B*) Haploid (*n*) or diploid homozygous (2*n*) *pol3Δ ura7Δ* mutants expressing either WT *POL3* or mutant *pol3-01*, were grown as in *A*. (*C*) Proliferation curves. Diploid homozygous *pol3Δ* or *pol3Δ ura7Δ* strains were transformed with either WT *POL3* or *pol3-01* plasmids. Three independent isogenic strains for each genotype were grown overnight in YPD and diluted next day to $OD_{600} = 0.1$ in fresh YPD. Proliferation was followed by OD_{600} measurements, and the values were plotted as mean ± SD on $\log_2$ scale. (*D*) Quantification of *CAN1* inactivation rates in diploid strains hemizygous for *CAN1* locus (see *SI Materials and Methods* for additional details) and homozygous for *pol3Δ* or *pol3Δ ura7Δ* mutations complemented with *POL3* or *pol3-01* plasmids. Error bars represent the 95% confidence intervals (CIs) and numbers on top indicate the fold increase in the mutation rate over the WT diploid strain (2.4 × 10^{-7} Can^R mutants per cell division).

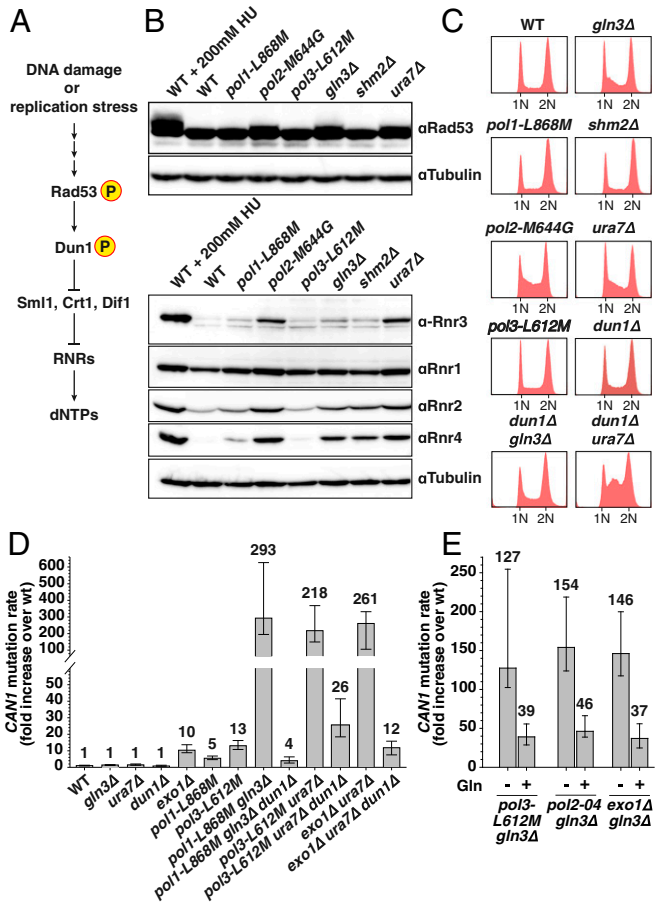

Fig. 3. Inactivation of Ura7 or Gln3 results in DDR checkpoint activation. (*A*) Simplified diagram depicting DDR response in *S. cerevisiae*. (*B*) Whole-cell lysates of logarithmically growing cells were analyzed by Western blotting with Rad53 and RNR1-4 antibodies. WT cells treated with 200 mM hydroxyurea (HU) were used as control for activation of DDR. (*C*) DNA content profiles of the indicated strains. (*D*) Mutation rates in mutant strains in the presence or absence of *DUN1*. See also Table S3. (*E*) Mutation rates in the indicated strains grown in YPD media supplemented or not with 5 mM glutamine (Gln). Error bars represent the 95% CI, and numbers on top indicate the fold increase in the mutation rate over WT.

exo1Δ ura7Δ double mutant also reduced the *CAN1* mutation rate up to *exo1Δ* levels (from 261-fold to 12-fold over WT) (Fig. 3*D*). Thus, the gain in DNA replication fidelity observed in the absence of *DUN1* is not restricted to strains carrying DNA polymerase mutant alleles, and it is likely a consequence of reduced dNTP concentrations. On the other hand, Dun1 inactivation enhanced the S-phase delay observed in *ura7Δ* (and had no effect in *gln3Δ* mutant) as indicated by DNA content analysis (Fig. 3*C*).

Gln3, a member of the GATA transcription factor family negatively regulated by target of rapamycin (TOR), activates genes subject to nitrogen catabolite repression, particularly during glutamine limitation (63). Glutamine is an energy source and a substrate for the synthesis of purines and pyrimidines, among other nitrogen-containing molecules (39, 64). Thus, we tested whether supplementation of the culture media (YPD) with 5 mM glutamine can suppress the mutator phenotype of *pol3-L612M gln3Δ*, *pol2-04 gln3Δ*, and *exo1Δ gln3Δ* double mutants. Remarkably, glutamine supplementation resulted in a partial 3.3-, 3.3-, and 4-fold reduction in the *CAN1* mutation rates, respectively (Fig. 3*E*). These observations suggest that, although *gln3Δ* cells were grown in rich media, at later stages during the growth of the culture, glutamine becomes limited resulting in increased mutagenesis.

Gln3 and Ura7 Are Both Required for Maintenance of Normal dNTP Pools. Because deletion of *GLN3* and *URA7* both resulted in activation of DDR and both genes have metabolism-related functions, we hypothesized that their loss influences the balance of nucleotide pools. Quantification of ribonucleoside 5′-triphosphate (NTP) concentrations in these mutants (Fig. 4*A* and Table S4) revealed a 66% reduction in CTP levels in *ura7Δ*, which is in agreement with a previous report (37). Remarkably, *gln3Δ* also presented 46% reduction in CTP levels and a 1.7-fold increase in UTP pools. Because CTP is converted into CDP and then reduced by RNR into dCDP, which can be used for either dCTP or dTTP biosynthesis (Fig. 5*A*) (9), we tested whether lower CTP levels might affect dNTP pools. Strikingly, we found that *gln3Δ* and *ura7Δ* mutations both resulted in ∼50% reduction in dCTP levels and a concomitant increase in dTTP, dATP, and dGTP ranging from 2.4- up to 4-fold over their respective WT dNTP concentrations (Fig. 4*B*). In contrast, NTP and dNTP levels in *shm2Δ*, *pol1-L868M*, or *pol3-L612M* mutants were indistinguishable from WT strain (Fig. 4 *A* and *B* and Tables S4 and S5). In agreement with previous reports, we found that *pol2-M644G* mutant presents an overall increase in dNTP pools (60, 65).

Next, we measured NTP/dNTP levels in *dun1Δ gln3Δ* and *dun1Δ ura7Δ* double mutants (Fig. 4 *A* and *B*). Importantly, we found that, in the absence of Dun1, nucleotide pools in *gln3Δ* and *ura7Δ* strains were almost identical to WT, with exception of CTP and dCTP, which remained 30–50% and 64% lower, respectively. Therefore, Dun1 inactivation partially suppresses the dNTP imbalance in *ura7Δ* and *gln3Δ* mutants and consequently its mutagenic potential.

Inactivation of Gln3, Ura7, and Shm2 Causes an Increase in Mutations Dominated by C-to-T Transitions. To further characterize *ura7Δ*, *gln3Δ*, and *shm2Δ* mutants, we carried out mutational spectra analysis at the *CAN1* locus (in an *msh6Δ* background to prevent the correction of mispairs) aiming to correlate this information with dNTP levels. According to previous findings (33), we observed in *msh6Δ* mutant a higher proportion of base substitutions compared with the WT strain (92% versus 75%, respectively) (Table S6). Moreover, the percentage of base substitutions increased up to 99% in *msh6Δ gln3Δ*, *msh6Δ ura7Δ*, or *msh6Δ shm2Δ* double mutants. Noteworthy, ∼95% of the mutations in *msh6Δ gln3Δ* and *msh6Δ ura7Δ* were G:C-to-A:T transitions (compared with 54% observed in *msh6Δ*) (Fig. 4*C* and Table S6). A similar trend was also found in *msh6Δ shm2Δ* in which G:C-to-A:T transitions represented 80% of Can^R events.

Analysis of the mutation spectra in *msh6Δ gln3Δ* identified G788A, G806A, G980A, G1018A, and G1622A as mutational hotspots occurring at a frequency at least 3.5 times higher than in the *msh6Δ* strain and two other weaker hotspots (G584A and C1426T) (Fig. 4*D* and Table S7). Comparing the mutation spectra in *msh6Δ gln3Δ* with *msh6Δ ura7Δ* revealed interesting similarities including hotspots G584A, G788A, G980A, G1018A, and C1426T. However, in *msh6Δ ura7Δ*, only G670A and G788A hotspots are significantly different from *msh6Δ*. Interestingly, some of these mutations, including G670A, G788A, and G980A, were also found in *msh6Δ shm2Δ* (Table S7), although this mutant in general had a broader distribution of the G:C-to-A:T transitions across the *CAN1* gene. The increased frequency of G:C-to-A:T transitions in *msh6Δ gln3Δ* and *msh6Δ ura7Δ* strains is in agreement with the reduced dCTP and elevated dTTP levels, resulting in a dCTP:dTTP ratio of 1:15 compared with the 1:2 ratio existing in WT cells. We also identified one mutational hotspot (G497A) preferentially found in strains with normal dCTP levels (*msh6Δ* and *msh6Δ shm2Δ*) (Fig. 4*E*). Thus, this mutation appears to be counterselected in strains with reduced dCTP levels, given the sequence context that demands dCTP, immediately after the predicted dTTP misincorporation.

Discussion

Gln3, Shm2, Ura7, and Exo1 Increase Lagging-Strand DNA Replication Fidelity. We discovered that, like *EXO1* deletion, the inactivation of *GLN3*, *URA7*, and *SHM2* caused synergistic increases in mutation rates exclusively in combination with lagging-strand DNA polymerase active-site mutant alleles (*pol1-L868M* or *pol3-L612M*).

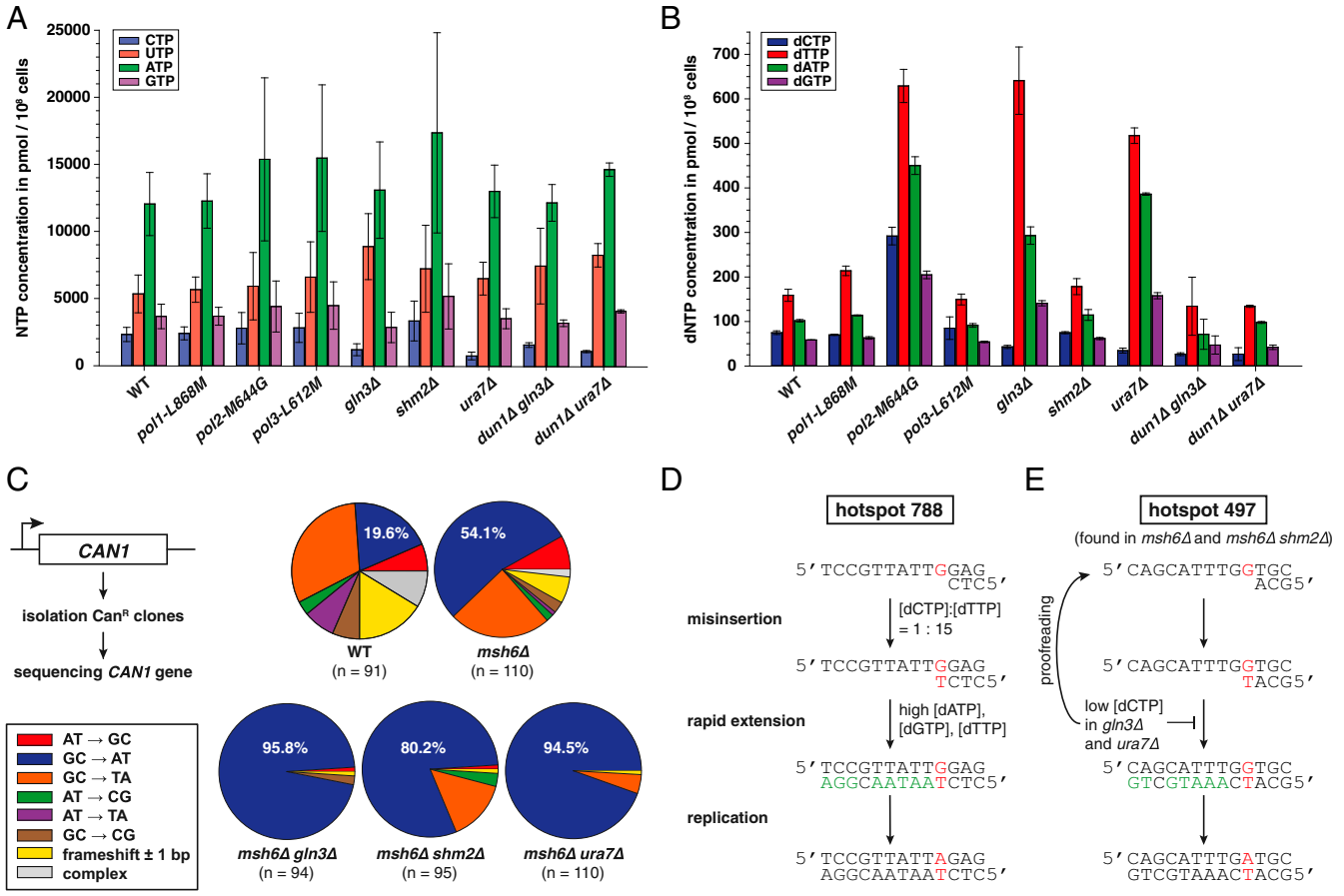

Fig. 4. Inactivation of Gln3 or Ura7 results in NTP and dNTP imbalance causing increased G:C-to-A:T transitions. (*A*) NTP and (*B*) dNTP pool measurements in the indicated strains (Tables S4 and S5). Error bars represent SD. (*C*) Independent Can^R clones ($n \geq 91$ per genotype) were sequenced for *CAN1* mutations. Graphs indicate the type of identified mutations, in percentages (see also Tables S6 and S7). (*D*) The G-to-A mutational hotspot at nucleotide 788 was frequently found in *msh6Δ gln3Δ*, m*sh6Δ shm2Δ*, and *msh6Δ ura7Δ* strains. Predicted mutation is noted in red. Nucleotides marked in green are facilitating mispair rapid extension prior proofreading due to their higher abundance in *gln3Δ* or *ura7Δ* mutants, compared with the WT strain. (*E*) The G-to-A mutational hotspot at position 497 was frequently found in *msh6Δ* and *msh6Δ shm2Δ*, but not in *msh6Δ gln3Δ* and *msh6Δ ura7Δ*. Here, the predicted G-dT mispair is immediately followed by incorporation of dCTP (in black), which is less abundant in *gln3Δ* and *ura7Δ* strains and, therefore, unlikely to support mispair rapid extension.

These findings contrast with the synergistic increase in mutation rates reported after introducing an *msh2Δ* mutation in either leading (*pol2-M644G*)- or lagging (*pol3-L612M*)-strand DNA polymerase mutant backgrounds (26). There are several possible explanations for this Polδ/lagging-strand bias: (*i*) a higher DNA replication fidelity during leading-strand synthesis facilitated by Polε checkpoint activation (66–68), which might provide additional time for proofreading or MMR; (*ii*) an increased base selectivity of Polε (by a factor of 10) compared with Polδ (2); (*iii*) intrinsic differences of how these active-site mutations interfere with Polε and Polδ replication fidelity; or (*iv*) leading- and lagging-strand DNA synthesis being mainly done by Polδ. This fourth hypothesis, supported by a recent study (69), opened up a strong controversy about the assignment of replicative DNA polymerases to the leading- or lagging-strand synthesis (70). At this point, we cannot distinguish between these different possibilities. However, it is interesting that *ura7Δ* and *gln3Δ* mutants showed remarkable similarities to a previously reported *rnr1* mutant (*rnr1-Q288A*), which causes altered dNTP pools and increased mutagenesis (68). Similar to *ura7Δ* or *gln3Δ*, *rnr1-Q288A* shows reduced dCTP pools, resulting in the same dCTP:dTTP = 1:15 ratio, and activation of the DDR. Moreover, *rnr1-Q288A CAN1* mutation spectra contained several hotspots (G670A, G788A, and G1018A) frequently found in *msh6Δ ura7Δ* (some of them also present in *msh6Δ gln3Δ*). Notably, mutational hotspots identified in the *rnr1-Q288A* strain were predicted as a consequence of lagging-strand replication. Thus, the bias for lagging-strand mutagenesis, observed in *gln3Δ*, *ura7Δ*, and *rnr1-Q288A* mutant strains, might be explained by inadequate dNTP pools causing S-phase checkpoint activation during Polε's leading-strand synthesis. In this way, checkpoint activation might provide additional time for polymerase proofreading and/or MMR. Future studies will be required to investigate why most of the mutations identified here show a mutator bias for active-site mutants of lagging-strand DNA polymerases.

Rrm3 and Shm2 Contribute to DNA Replication Fidelity. The Rrm3 helicase facilitates the passage through natural pausing sites of genomic regions containing replication fork barriers (42, 43, 51). Similarly, Rrm3 could facilitate the passage through DNA pausing sites resulting from low-fidelity DNA replication conditions, and therefore be preferentially required for polymerases with high processivity (Polε and Polδ) (71). Alternatively, the elevated dNTP pools in *rrm3Δ* mutant (72, 73) might promote mutagenesis, as it has been described for other mutations causing increased dNTP pools (74, 75). Moreover, a recent publication described an alternative helicase-independent Rrm3 function required for restricting DNA replication under replication stress (76), which could potentially enhance DNA replication fidelity. Future studies will address whether the effects described here are dependent on Rrm3's helicase activity or perhaps related to this alternative role of Rrm3.

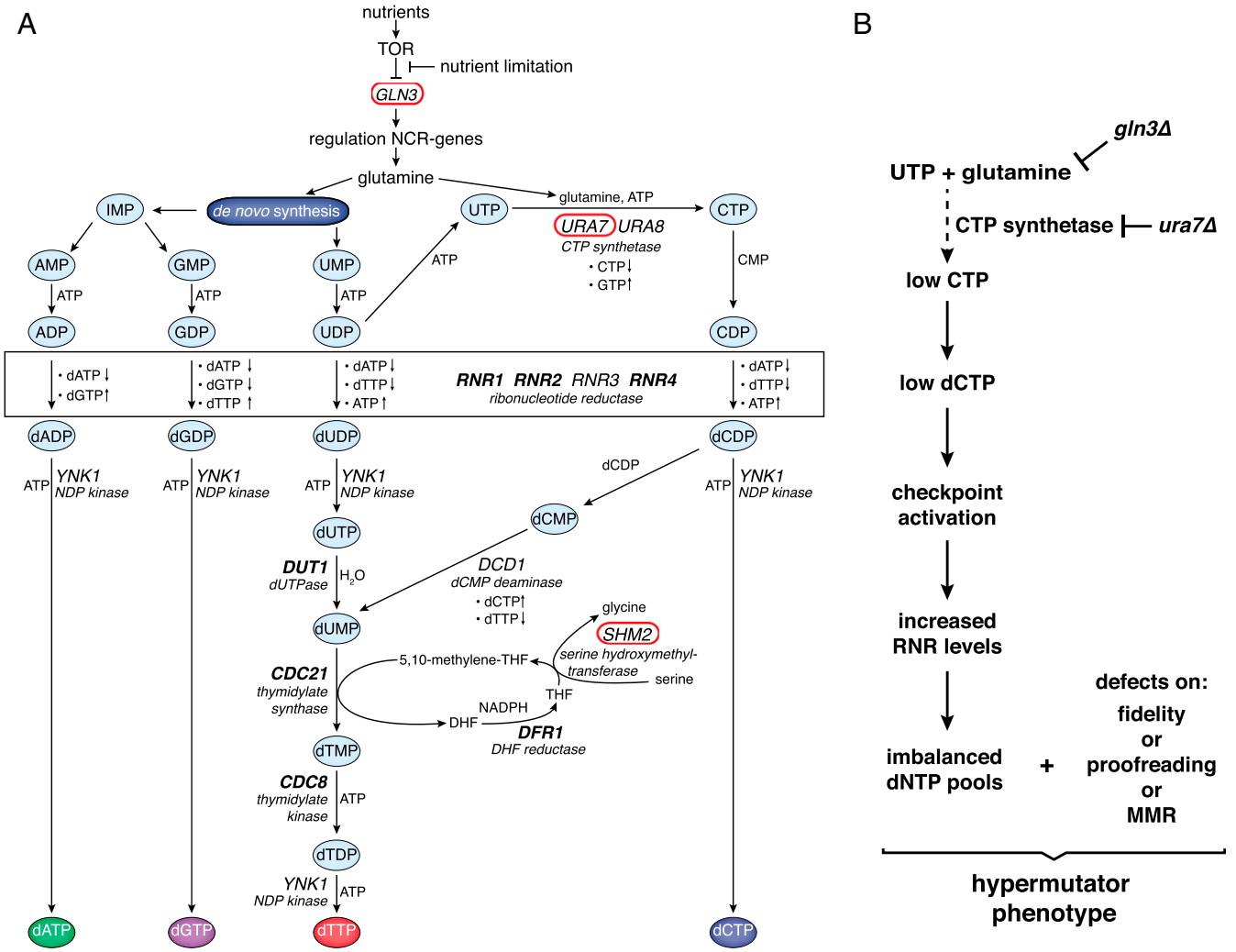

Fig. 5. (*A*) Pathways of de novo dNTP biosynthesis in *S. cerevisiae* (adapted from ref. 9). Essential genes are shown in bold (*RNR1*, *2*, and *4* are nonessential in certain yeast genetic backgrounds). Metabolism-related genes (*GLN3*, *URA7*, and *SHM2*) identified in this screen were encircled in red. (*B*) Gln3 and Ura7 promote DNA replication fidelity by preventing dNTP pool imbalances. Inactivation of Gln3 or Ura7 results in low CTP/dCTP levels, triggering DNA damage checkpoint activation. Up-regulation of RNR subunits, instead of compensating low dCTP pools, creates a severe dNTP pool imbalance that, in combination with altered DNA polymerase functions or partial MMR defects, causes severe mutator phenotypes.

Shm2 is a cytosolic serine hydroxymethyltransferase that synthesizes 5,10-methylene-tetrahydrofolate (5,10-CH_2-THF) (40, 41), an intermediate in the one-carbon (C1) cycle and precursor in de novo synthesis of purines and pyrimidines (Fig. 5*A*). In mammals, the same reaction is catalyzed by the serine hydroxymethyltransferase 1 (Shmt1) (Shmt1 is the mammalian homolog of yeast Shm2). Mammalian Shmt1 also serves as a scaffold protein that facilitates the interaction with DHFR and thymidylate synthase at the nuclear lamina (77). Remarkably, inactivation of Shmt1 in mice (78, 79) or its down-regulation in human lung cells (80) results in increased uracil incorporation into DNA as result of impaired de novo dTMP biosynthesis.

Here, we found that inactivation of Shm2 results in increased mutation rates in DNA polymerase mutant backgrounds (*pol1-L868M*, *pol3-L612M*, or *pol2-04*) (Tables 1 and 2) but not when MMR has been inactivated (*msh2Δ* strain) (Table S3). These observations indicate that the type of damage generated in the absence Shm2 is not repaired by MMR and does not causes mutagenesis unless DNA polymerase function is affected.

Because Shm2 generates 5,10-CH_2-THF, which is used as cofactor during nucleotide biosynthesis, we hypothesized that loss of Shm2 might cause dNTP pool imbalances and consequently DNA replication infidelity. Interestingly, inactivation of Shm2 in *S. cerevisiae* neither caused alterations in NTP or dNTP pools (Fig. 4 *A* and *B* and Tables S4 and S5) nor resulted in activation of the DDR (Fig. 3 *B* and *C*), which otherwise is a common feature described for mutants with dNTP pools below their normal level (81). One possible explanation is that loss of Shm2 results in increased oxidative damage, leading to modified cytosine or uracil bases, which upon incorporation into DNA might be susceptible to deamination events frequently associated with C-to-T transitions. Supporting this hypothesis, quantitative metabolic flux analysis done in mammalian cells revealed that the C1 cycle, through oxidation of 5,10-CH_2-THF, contributes to the production ∼40% of NADPH (82), a central cofactor in redox homeostasis. Alternatively, loss of Shm2 in *S. cerevisiae*, similar to inactivation of mammalian Shmt1 (78, 80), might cause uracil accumulation and increased mutagenesis. However, our analysis in *shm2Δ* mutants did not reveal major differences in NTP/dNTP pools or signs of DDR activation. Thus, if loss of Shm2 causes dUTP accumulation in *S. cerevisiae*, this increase might have been below our limit of detection, but nevertheless sufficient to cause genome instability.

Low dCTP Levels as an Achilles' Heel of High-Fidelity DNA Replication. Among the mutants identified here, both *ura7Δ* and *gln3Δ* showed the strongest mutator synergies with DNA polymerases

or MMR mutant alleles (Tables 1 and 2 and Table S3). Although inactivation of Gln3 or Ura7 (in an *msh6Δ* background) mainly resulted in base substitutions (Fig. 4*C* and Table S6), we also found a small increase in frameshift mutations in combination with *msh6Δ* or *exo1Δ*, but not with *msh3Δ* or *msh2Δ* backgrounds (Table S3). We propose that this increase in frameshifts is not directly associated to the dNTP imbalance caused by *gln3Δ* and *ura7Δ* mutations, but rather a consequence of an overload of MMR capacity due to a large quantity of base substitutions, thus preventing the recognition of frameshifts.

Previous reports demonstrated that Ura7 contributes to a great extent (~80%) to the production of CTP (a minor isoform called Ura8 gives account for the remaining CTP production) (37). However, the potential consequences of reduced CTP levels on dNTP pools remained unknown. We found that loss of Ura7 not only affects CTP pools but also results in a 50% reduction in dCTP pools with a concomitant increase in the concentration of the other three dNTPs (Fig. 4 *A* and *B* and Tables S4 and S5).

The role of the transcription factor Gln3 in NTP/dNTP pool maintenance has not been previously investigated. Here, we provide evidence that, although glutamine is used for de novo synthesis of both purines and pyrimidines, loss of Gln3 under our experimental conditions preferentially affects CTP and dCTP concentrations. Similar to *ura7Δ* mutant, the *gln3Δ* strain had a 50% reduction in CTP and dCTP levels as well as higher levels on the other dNTPs (Fig. 4 *A* and *B* and Tables S4 and S5). Importantly, we demonstrated that the strong mutator phenotype of *gln3Δ* double mutants was largely suppressed by glutamine supplementation (Fig. 3*E*). Glutamine is used as nitrogen source for protein and nucleotide biosynthesis and is considered one important "fuel" for cancer cells. This is illustrated by the fact that some cancer cell lines are strongly dependent on external glutamine for survival ("glutamine addiction") (64, 83). Consequently, glutamine analogs inhibit cell proliferation, in part by inactivating glutamine-requiring enzymes involved in purine and pyrimidine biosynthesis (including CTP synthetase). Moreover, the glutamine analog *Acivicin*, which strongly inhibits CTP synthetase activity (84), has been shown to induce a dNTP imbalance characterized by reduced CTP/dCTP levels and increased UTP levels (85, 86), which is reminiscent of the *gln3Δ* mutant phenotype. In light of our findings, it would be interesting to investigate whether a low glutamine environment, as recently described for the core region in solid tumors (87) or due to glutamine analog treatment, causes increased mutagenesis, accelerating tumor evolution and the acquisition of cancer drug resistance.

The finding that deletion of *DUN1* suppresses the strong mutator phenotype of double mutants carrying *ura7Δ* or *gln3Δ* mutations in DNA replication fidelity-compromised backgrounds (Fig. 3*D*), suggests that this phenotype is in part caused by DDR activation. This hypothesis is further supported by the finding that suppression of the mutator phenotype upon *DUN1* deletion correlates with a reduction in dATP, dTTP, and dGTP levels (Fig. 4*B*), resulting in a dNTP pool with less mutagenic potential given the lower dTTP: dCTP ratio. The differences between *dun1Δ ura7Δ* and *dun1Δ gln3Δ* DNA content profiles (Fig. 3*C*) are consistent with a major role of Ura7 during CTP synthesis, whereas Gln3 is required under special circumstances (e.g., glutamine limitation). We speculate that conditions restricting dNTPs biosynthesis (e.g., *dun1Δ*) will prevent depletion of glutamine pools, and consequently cells might not heavily rely on Gln3 functions.

RNR catalytic activity responds to sophisticated allosteric regulation that "senses" three out of the four dNTPs (RNR is refractory to dCTP levels) and can "fine-tune" them, according to the cellular demands (Fig. 5*A*) (88). Excess in dCDP pools can be redirected to the synthesis of dTTPs by the action of dCMP deaminase. However, cells are not able to compensate for reductions in dCTP pools. As illustrated in Fig. 5*B*, *ura7Δ* or *gln3Δ* mutation interferes with the production of CTP, which is used as substrate for dCTP biosynthesis. Reduced dCTP levels likely cause stalled replication forks and activation of the DDR, which, instead of compensating for low dCTP levels, creates a severe dNTP imbalance with high mutagenic potential.

Mutation spectra analysis in *gln3Δ* or *ura7Δ* mutants revealed a strong increase in G:C-to-A:T transitions, representing about 95% of the identified mutations (Fig. 4*C* and Table S7). The reduced dCTP and high dTTP levels observed in *gln3Δ* or *ura7Δ* mutants are likely driving the misincorporation of dTTP at positions where dCTP would be required.

Without any exception, all mutational hotspots identified in this study can be explained by the "next-nucleotide effect" (8, 89). According to this model, after the misincorporation of a nucleotide, the high concentration of the next nucleotide (given by the sequence context) favors its incorporation (rapid extension) before proofreading of the previously misincorporated nucleotide (Fig. 4 *D* and *E* and Table S7). For example, at G788A transition, which occurs 16 times more frequently in *msh6Δ ura7Δ* compared with *msh6Δ*, the predicted T misincorporation (resulting in a G-dT mispair) is followed by the correct incorporation of 5 nt, in which none of them is C, and all nucleotides are at least 2.7-fold more abundant than in the WT strain (Fig. 4*D*). The same holds true for other hotspots, with some variations in the number of nucleotides that are introduced after the mispaired base, until the next C is required.

The characterization of mammalian cell lines resistant to inhibitory concentrations of specific nucleosides (or their analogs) (90, 91) revealed that mutations affecting the allosteric regulation of key enzymes involved in dNTP biosynthesis (RNR, CTP synthetase, and dCMP deaminase) can lead to dNTP imbalances, and in some cases, increased mutator phenotypes. Consequently, the identification and characterization of genes affecting dNTP pools might provide insights into mutagenesis and cancer susceptibility. Unfortunately, quantification of dNTP pools is laborious and not well suited for high-content screening. Therefore, this type of analysis has been limited to a relatively small number of gene mutations. In addition, not all dNTP imbalances correlate with increased mutation rates. For example, inactivation of dCMP deaminase (*dcd1Δ*) in *S. cerevisiae* resulted in 3-fold reduction in dTTP pool and about 30-fold increased in dCTP levels, without any consequences on mutation rates at the *URA4* reporter (92).

Future studies will be required to understand in more detail the consequences of dNTP imbalances and S-phase checkpoint activation on DNA replication fidelity. As it has been suggested by Kumar et al. (81), a collection of strains with diverse well-defined dNTP pool imbalances would be extremely useful to expand our understanding how dNTP imbalances and checkpoint activation affect DNA replication fidelity.

In summary, we uncovered a group of previously unrecognized genes (*GLN3*, *SHM2*, *RRM3*, and *URA7*) that contribute to DNA replication fidelity. Two of these mutations (*gln3Δ* and *ura7Δ*) caused imbalanced dNTP pools by preventing the production of substrates used by RNR for dNTP biosynthesis. Importantly, these dNTP imbalances, when combined with partial defects on DNA polymerase functions or MMR activity, cause severe mutator phenotypes. In light of these observations, it is likely that still-unrecognized mutations (or environmental conditions) might influence the balance of dNTPs without immediate consequences on mutation rates. Such mutations or conditions can have dramatic effects on mutation rates when combined with defects in other DNA replication fidelity determinants often found in cancer cells. Therefore, our results not only highlight the superb buffer capabilities of the eukaryotic DNA replication and MMR system, but they also open up avenues to investigate genetic interactions that might drive mutator phenotypes and potentially tumor evolution. Thus, the human counterparts of the genes identified here could represent potential "minidrivers" for cancer development, which might participate in polygenic interactions resulting in increased mutagenesis.

Materials and Methods

All *S. cerevisiae* strains used in this study (Table S8) were derivatives of the S288C strains RDKY3686 (MATα *ura3-52 leu2Δ1 trp1Δ63 hom3-10 his3Δ200 lys2-10A*)

(93) or RDKY5964 (a MATa version of RDKY3686) (26). Strains were cultivated at 30 °C according to standard protocols. Gene deletions and gene tagging were performed using standard PCR-based recombination methods (94), followed by confirmation by PCR. Correct insertion of tags or point mutations, as well as absence of additional unwanted mutations, were confirmed by sequencing. Specific mutations (*pol1-L868M*, *pol2-M644G*, *pol3-L612M*, *pol2-04*, *cyh2-Q38K*) were introduced at the chromosomal locus by pop-in/pop-out or PCR-based recombination methods and the presence of the desired mutations, as well as the absence of additional mutations, was confirmed by sequencing (for details, see *SI Materials and Methods*).

Genome-Wide Screen in *S. cerevisiae*. Here, we engineered a modified version of the SGA protocol (32) to cross (using a RoToR robot; Singer Instruments) the nonessential gene deletion collection (BY4742) (MATα *his3Δ1 leu2Δ0 ura3Δ lys2Δ yfg::kanMX4*) with four queries (HHY5298, HHY5292, HHY5984, and HHY5289), carrying the wt-*POL1*, *pol1-L868M*, *pol2-M644G*, or *pol3-L612M* alleles, respectively [marked with a nourseothricin (nat) cassette at the 3′-UTR]. Otherwise, all four queries shared the following genotype: MATa *ura3-52 leu2Δ1 trp1Δ63 his3Δ200 cyh2-Q38K hom3-10.HIS3 pMFA1-klLEU2. hphNT1.lys2-10A MLH2.klURA3*, which allowed the systematic mating, sporulation, and selection procedure (for details about query strain construction and SGA modifications, see *SI Materials and Methods*).

For qualitative mutator analysis, double-mutant cells were spotted on YPD-agar using Liquidator 96 (Mettler Toledo) and grown for 2 d at 30 °C. Next, plates were imaged using the GelDoc system (Bio-Rad) and replica plated onto two different mutator reporter plates, either lacking lysine (*lys2-10A* frameshift reversion assay) or containing canavanine (*CAN1* inactivation assay), and grown for 4 d at 30 °C. Plates were imaged for documentation and scored visually. Positive hits were rechecked and those double mutants that showed increased mutator phenotype were generated in RDKY5964 (or RDKY3686) for further analysis.

Determination of Mutation Rates. Mutation rates using frameshift reversion assays (*hom3-10* and *lys2-10A*) and the *CAN1* inactivation assay were determined by fluctuation analysis as previously described (33, 93). *URA3* forward inactivation rates were similarly determined by fluctuation analysis based on the spontaneous appearance of 5-fluoroorotic acid (5-FOA)-resistant colonies. Each mutation rate was determined by using two biological isolates and at least 14 independent cultures.

Yeast Cell Lysates and Immunoblotting. *S. cerevisiae* whole-cell protein extracts were generated as previously described (26) and were analyzed on 7% or 8% SDS/PAGE followed by immunoblotting using anti-Rad53 (EL7.E1; Abcam), anti-Rnr1 (AS09576; Agrisera), anti-Rnr2 (AS09575; Agrisera), and anti-Rnr3 (AS09574; Agrisera). YL1/2 antibody (Sigma) was used to probe for Rnr4 and tubulin (81).

DNA Content Analysis. Logarithmic *S. cerevisiae* cultures were processed as described in ref. 6 and analyzed using BD FACSCanto II (BD Biosciences).

Determination of NTP and dNTP Pools. NTP and dNTPs were measured as described (60).

***CAN1* Mutation Spectra Analysis.** The *CAN1* gene from individual Can^R clones was amplified from genomic DNA by PCR and sequenced (GATC Biotech). Sequences were analyzed with Lasergene 12 (DNASTAR). Mutation spectra distributions and mutational hotspots were compared with Fisher's exact test in R. Values of $P \leq 0.05$ were defined as significantly different.

ACKNOWLEDGMENTS. We thank Adam J. Rose, Hannah Zhao, Alhassan Abdelsamie, and N. Katarina Horvat for critical reading of this manuscript. Thanks to Richard D. Kolodner for helpful discussions, strains, and reagents. Also, we are grateful to Christopher D. Putnam and Linda Reha-Krantz for valuable discussions and to Tobias P. Dick for sharing reagents. Thanks to Annette Kopp-Schneider for advice on statistical analysis and to Frank Exner for technical support. This work was supported by the German Cancer Research Center and the Marie Curie Career Integration Grant "iMMR" (granted to H.H.), and by the Swedish Cancer Society, the Knut and Alice Wallenberg Foundation, and the Swedish Research Council (granted to A.C.).

1. Ganai RA, Johansson E (2016) DNA replication—a matter of fidelity. *Mol Cell* 62: 745–755.
2. St Charles JA, Liberti SE, Williams JS, Lujan SA, Kunkel TA (2015) Quantifying the contributions of base selectivity, proofreading and mismatch repair to nuclear DNA replication in *Saccharomyces cerevisiae*. *DNA Repair (Amst)* 31:41–51.
3. Kunkel TA (2009) Evolving views of DNA replication (in)fidelity. *Cold Spring Harb Symp Quant Biol* 74:91–101.
4. Reyes GX, Schmidt TT, Kolodner RD, Hombauer H (2015) New insights into the mechanism of DNA mismatch repair. *Chromosoma* 124:443–462.
5. Kunkel TA, Erie DA (2015) Eukaryotic mismatch repair in relation to DNA replication. *Annu Rev Genet* 49:291–313.
6. Hombauer H, Srivatsan A, Putnam CD, Kolodner RD (2011) Mismatch repair, but not heteroduplex rejection, is temporally coupled to DNA replication. *Science* 334: 1713–1716.
7. Aksenova A, et al. (2010) Mismatch repair-independent increase in spontaneous mutagenesis in yeast lacking non-essential subunits of DNA polymerase ε. *PLoS Genet* 6:e1001209.
8. Reha-Krantz LJ (2010) DNA polymerase proofreading: Multiple roles maintain genome stability. *Biochim Biophys Acta* 1804:1049–1063.
9. Mathews CK (2015) Deoxyribonucleotide metabolism, mutagenesis and cancer. *Nat Rev Cancer* 15:528–539.
10. Reichard P (2010) Ribonucleotide reductases: Substrate specificity by allostery. *Biochem Biophys Res Commun* 396:19–23.
11. Elledge SJ, Davis RW (1987) Identification and isolation of the gene encoding the small subunit of ribonucleotide reductase from *Saccharomyces cerevisiae*: DNA damage-inducible gene required for mitotic viability. *Mol Cell Biol* 7:2783–2793.
12. Huang M, Elledge SJ (1997) Identification of RNR4, encoding a second essential small subunit of ribonucleotide reductase in *Saccharomyces cerevisiae*. *Mol Cell Biol* 17: 6105–6113.
13. Elledge SJ, Davis RW (1990) Two genes differentially regulated in the cell cycle and by DNA-damaging agents encode alternative regulatory subunits of ribonucleotide reductase. *Genes Dev* 4:740–751.
14. Serero A, Jubin C, Loeillet S, Legoix-Né P, Nicolas AG (2014) Mutational landscape of yeast mutator strains. *Proc Natl Acad Sci USA* 111:1897–1902.
15. Lang GI, Parsons L, Gammie AE (2013) Mutation rates, spectra, and genome-wide distribution of spontaneous mutations in mismatch repair deficient yeast. *G3 (Bethesda)* 3:1453–1465.
16. Lujan SA, et al. (2014) Heterogeneous polymerase fidelity and mismatch repair bias genome variation and composition. *Genome Res* 24:1751–1764.
17. Palles C, et al.; CORGI Consortium; WGS500 Consortium (2013) Germline mutations affecting the proofreading domains of POLE and POLD1 predispose to colorectal adenomas and carcinomas. *Nat Genet* 45:136–144.
18. Rayner E, et al. (2016) A panoply of errors: Polymerase proofreading domain mutations in cancer. *Nat Rev Cancer* 16:71–81.
19. Lynch HT, de la Chapelle A (2003) Hereditary colorectal cancer. *N Engl J Med* 348: 919–932.
20. Lujan SA, Williams JS, Kunkel TA (2016) DNA polymerases divide the labor of genome replication. *Trends Cell Biol* 26:640–654.
21. Nick McElhinny SA, Gordenin DA, Stith CM, Burgers PM, Kunkel TA (2008) Division of labor at the eukaryotic replication fork. *Mol Cell* 30:137–144.
22. Pursell ZF, Isoz I, Lundström EB, Johansson E, Kunkel TA (2007) Yeast DNA polymerase epsilon participates in leading-strand DNA replication. *Science* 317:127–130.
23. Pavlov YI, Mian IM, Kunkel TA (2003) Evidence for preferential mismatch repair of lagging strand DNA replication errors in yeast. *Curr Biol* 13:744–748.
24. Nick McElhinny SA, Kissling GE, Kunkel TA (2010) Differential correction of lagging-strand replication errors made by DNA polymerases alpha and delta. *Proc Natl Acad Sci USA* 107:21070–21075.
25. Goellner EM, Putnam CD, Kolodner RD (2015) Exonuclease 1-dependent and independent mismatch repair. *DNA Repair (Amst)* 32:24–32.
26. Hombauer H, Campbell CS, Smith CE, Desai A, Kolodner RD (2011) Visualization of eukaryotic DNA mismatch repair reveals distinct recognition and repair intermediates. *Cell* 147:1040–1053.
27. Liberti SE, Larrea AA, Kunkel TA (2013) Exonuclease 1 preferentially repairs mismatches generated by DNA polymerase α. *DNA Repair (Amst)* 12:92–96.
28. Morrison A, Johnson AL, Johnston LH, Sugino A (1993) Pathway correcting DNA replication errors in *Saccharomyces cerevisiae*. *EMBO J* 12:1467–1473.
29. Tran HT, Gordenin DA, Resnick MA (1999) The 3′→5′ exonucleases of DNA polymerases delta and epsilon and the 5′→3′ exonuclease Exo1 have major roles in post-replication mutation avoidance in *Saccharomyces cerevisiae*. *Mol Cell Biol* 19: 2000–2007.
30. Williams LN, Herr AJ, Preston BD (2013) Emergence of DNA polymerase ε antimutators that escape error-induced extinction in yeast. *Genetics* 193:751–770.
31. Herr AJ, et al. (2011) Mutator suppression and escape from replication error-induced extinction in yeast. *PLoS Genet* 7:e1002282.
32. Tong AH, Boone C (2006) Synthetic genetic array analysis in *Saccharomyces cerevisiae*. *Methods Mol Biol* 313:171–192.
33. Marsischky GT, Filosi N, Kane MF, Kolodner R (1996) Redundancy of *Saccharomyces cerevisiae* MSH3 and MSH6 in MSH2-dependent mismatch repair. *Genes Dev* 10: 407–420.
34. Brusky J, Zhu Y, Xiao W (2000) UBC13, a DNA-damage-inducible gene, is a member of the error-free postreplication repair pathway in *Saccharomyces cerevisiae*. *Curr Genet* 37:168–174.
35. Huang ME, Rio AG, Nicolas A, Kolodner RD (2003) A genomewide screen in *Saccharomyces cerevisiae* for genes that suppress the accumulation of mutations. *Proc Natl Acad Sci USA* 100:11529–11534.

36. Ozier-Kalogeropoulos O, Fasiolo F, Adeline MT, Collin J, Lacroute F (1991) Cloning, sequencing and characterization of the *Saccharomyces cerevisiae* URA7 gene encoding CTP synthetase. *Mol Gen Genet* 231:7–16.
37. Ozier-Kalogeropoulos O, Adeline MT, Yang WL, Carman GM, Lacroute F (1994) Use of synthetic lethal mutants to clone and characterize a novel CTP synthetase gene in *Saccharomyces cerevisiae*. *Mol Gen Genet* 242:431–439.
38. Cooper TG (2002) Transmitting the signal of excess nitrogen in *Saccharomyces cerevisiae* from the Tor proteins to the GATA factors: Connecting the dots. *FEMS Microbiol Rev* 26:223–238.
39. Ljungdahl PO, Daignan-Fornier B (2012) Regulation of amino acid, nucleotide, and phosphate metabolism in *Saccharomyces cerevisiae*. *Genetics* 190:885–929.
40. McNeil JB, et al. (1994) Cloning and molecular characterization of three genes, including two genes encoding serine hydroxymethyltransferases, whose inactivation is required to render yeast auxotrophic for glycine. *J Biol Chem* 269:9155–9165.
41. Kastanos EK, Woldman YY, Appling DR (1997) Role of mitochondrial and cytoplasmic serine hydroxymethyltransferase isozymes in de novo purine synthesis in *Saccharomyces cerevisiae*. *Biochemistry* 36:14956–14964.
42. Azvolinsky A, Giresi PG, Lieb JD, Zakian VA (2009) Highly transcribed RNA polymerase II genes are impediments to replication fork progression in *Saccharomyces cerevisiae*. *Mol Cell* 34:722–734.
43. Mohanty BK, Bairwa NK, Bastia D (2006) The Tof1p–Csm3p protein complex counteracts the Rrm3p helicase to control replication termination of *Saccharomyces cerevisiae*. *Proc Natl Acad Sci USA* 103:897–902.
44. Tran PT, Erdeniz N, Symington LS, Liskay RM (2004) EXO1—a multi-tasking eukaryotic nuclease. *DNA Repair (Amst)* 3:1549–1559.
45. Keijzers G, Liu D, Rasmussen LJ (2016) Exonuclease 1 and its versatile roles in DNA repair. *Crit Rev Biochem Mol Biol* 51:440–451.
46. Goodman MF, Woodgate R (2013) Translesion DNA polymerases. *Cold Spring Harb Perspect Biol* 5:a010363.
47. Goellner EM, et al. (2014) PCNA and Msh2-Msh6 activate an Mlh1-Pms1 endonuclease pathway required for Exo1-independent mismatch repair. *Mol Cell* 55:291–304.
48. Morrison A, Bell JB, Kunkel TA, Sugino A (1991) Eukaryotic DNA polymerase amino acid sequence required for 3′→5′ exonuclease activity. *Proc Natl Acad Sci USA* 88:9473–9477.
49. Herr AJ, Kennedy SR, Knowels GM, Schultz EM, Preston BD (2014) DNA replication error-induced extinction of diploid yeast. *Genetics* 196:677–691.
50. Koren A, Soifer I, Barkai N (2010) MRC1-dependent scaling of the budding yeast DNA replication timing program. *Genome Res* 20:781–790.
51. Ivessa AS, et al. (2003) The *Saccharomyces cerevisiae* helicase Rrm3p facilitates replication past nonhistone protein-DNA complexes. *Mol Cell* 12:1525–1536.
52. Rouse J, Jackson SP (2002) Interfaces between the detection, signaling, and repair of DNA damage. *Science* 297:547–551.
53. Tourrière H, Pasero P (2007) Maintenance of fork integrity at damaged DNA and natural pause sites. *DNA Repair (Amst)* 6:900–913.
54. Zhao X, Muller EG, Rothstein R (1998) A suppressor of two essential checkpoint genes identifies a novel protein that negatively affects dNTP pools. *Mol Cell* 2:329–340.
55. Chabes A, Domkin V, Thelander L (1999) Yeast Sml1, a protein inhibitor of ribonucleotide reductase. *J Biol Chem* 274:36679–36683.
56. Huang M, Zhou Z, Elledge SJ (1998) The DNA replication and damage checkpoint pathways induce transcription by inhibition of the Crt1 repressor. *Cell* 94:595–605.
57. Lee YD, Wang J, Stubbe J, Elledge SJ (2008) Dif1 is a DNA-damage-regulated facilitator of nuclear import for ribonucleotide reductase. *Mol Cell* 32:70–80.
58. Wu X, Huang M (2008) Dif1 controls subcellular localization of ribonucleotide reductase by mediating nuclear import of the R2 subunit. *Mol Cell Biol* 28:7156–7167.
59. Zhou Z, Elledge SJ (1993) DUN1 encodes a protein kinase that controls the DNA damage response in yeast. *Cell* 75:1119–1127.
60. Williams LN, et al. (2015) dNTP pool levels modulate mutator phenotypes of error-prone DNA polymerase ε variants. *Proc Natl Acad Sci USA* 112:E2457–E2466.
61. Datta A, et al. (2000) Checkpoint-dependent activation of mutagenic repair in *Saccharomyces cerevisiae* pol3-01 mutants. *Mol Cell* 6:593–603.
62. Mertz TM, Sharma S, Chabes A, Shcherbakova PV (2015) Colon cancer-associated mutator DNA polymerase δ variant causes expansion of dNTP pools increasing its own infidelity. *Proc Natl Acad Sci USA* 112:E2467–E2476.
63. Crespo JL, Powers T, Fowler B, Hall MN (2002) The TOR-controlled transcription activators GLN3, RTG1, and RTG3 are regulated in response to intracellular levels of glutamine. *Proc Natl Acad Sci USA* 99:6784–6789.
64. Wise DR, Thompson CB (2010) Glutamine addiction: A new therapeutic target in cancer. *Trends Biochem Sci* 35:427–433.
65. Nick McElhinny SA, et al. (2010) Genome instability due to ribonucleotide incorporation into DNA. *Nat Chem Biol* 6:774–781.
66. Navas TA, Zhou Z, Elledge SJ (1995) DNA polymerase epsilon links the DNA replication machinery to the S phase checkpoint. *Cell* 80:29–39.
67. Pursell ZF, Kunkel TA (2008) DNA polymerase epsilon: A polymerase of unusual size (and complexity). *Prog Nucleic Acid Res Mol Biol* 82:101–145.
68. Kumar D, et al. (2011) Mechanisms of mutagenesis in vivo due to imbalanced dNTP pools. *Nucleic Acids Res* 39:1360–1371.
69. Johnson RE, Klassen R, Prakash L, Prakash S (2015) A major role of DNA polymerase δ in replication of both the leading and lagging DNA strands. *Mol Cell* 59:163–175.
70. Burgers PM, Gordenin D, Kunkel TA (2016) Who is leading the replication fork, Pol ε or Pol δ? *Mol Cell* 61:492–493.
71. Reijns MA, et al. (2015) Lagging-strand replication shapes the mutational landscape of the genome. *Nature* 518:502–506.
72. Poli J, et al. (2012) dNTP pools determine fork progression and origin usage under replication stress. *EMBO J* 31:883–894.
73. O'Rourke TW, et al. (2005) Differential involvement of the related DNA helicases Pif1p and Rrm3p in mtDNA point mutagenesis and stability. *Gene* 354:86–92.
74. Chabes A, et al. (2003) Survival of DNA damage in yeast directly depends on increased dNTP levels allowed by relaxed feedback inhibition of ribonucleotide reductase. *Cell* 112:391–401.
75. Buckland RJ, et al. (2014) Increased and imbalanced dNTP pools symmetrically promote both leading and lagging strand replication infidelity. *PLoS Genet* 10:e1004846.
76. Syed S, Desler C, Rasmussen LJ, Schmidt KH (2016) A novel Rrm3 function in restricting DNA replication via an Orc5-binding domain is genetically separable from Rrm3 function as an ATPase/helicase in facilitating fork progression. *PLoS Genet* 12:e1006451.
77. Anderson DD, Woeller CF, Chiang EP, Shane B, Stover PJ (2012) Serine hydroxymethyltransferase anchors de novo thymidylate synthesis pathway to nuclear lamina for DNA synthesis. *J Biol Chem* 287:7051–7062.
78. Macfarlane AJ, Perry CA, McEntee MF, Lin DM, Stover PJ (2011) Shmt1 heterozygosity impairs folate-dependent thymidylate synthesis capacity and modifies risk of Apc(min)-mediated intestinal cancer risk. *Cancer Res* 71:2098–2107.
79. MacFarlane AJ, et al. (2008) Cytoplasmic serine hydroxymethyltransferase regulates the metabolic partitioning of methylenetetrahydrofolate but is not essential in mice. *J Biol Chem* 283:25846–25853.
80. Paone A, et al. (2014) SHMT1 knockdown induces apoptosis in lung cancer cells by causing uracil misincorporation. *Cell Death Dis* 5:e1525.
81. Kumar D, Viberg J, Nilsson AK, Chabes A (2010) Highly mutagenic and severely imbalanced dNTP pools can escape detection by the S-phase checkpoint. *Nucleic Acids Res* 38:3975–3983.
82. Fan J, et al. (2014) Quantitative flux analysis reveals folate-dependent NADPH production. *Nature* 510:298–302.
83. Hensley CT, Wasti AT, DeBerardinis RJ (2013) Glutamine and cancer: Cell biology, physiology, and clinical opportunities. *J Clin Invest* 123:3678–3684.
84. Weber G, et al. (1982) Multi-enzyme-targeted chemotherapy by acivicin and actinomycin. *Adv Enzyme Regul* 20:75–96.
85. Denton JE, Lui MS, Aoki T, Sebolt J, Weber G (1982) Rapid in vivo inactivation by acivicin of CTP synthetase, carbamoyl-phosphate synthetase II, and amidophosphoribosyltransferase in hepatoma. *Life Sci* 30:1073–1080.
86. Neil GL, Berger AE, McPartland RP, Grindey GB, Bloch A (1979) Biochemical and pharmacological effects of the fermentation-derived antitumor agent, (alphaS,5S)-alpha-amino-3-chloro-4,5-dihydro-5-isoxazoleacetic acid (AT-125). *Cancer Res* 39:852–856.
87. Pan M, et al. (2016) Regional glutamine deficiency in tumours promotes dedifferentiation through inhibition of histone demethylation. *Nat Cell Biol* 18:1090–1101.
88. Reichard P (1988) Interactions between deoxyribonucleotide and DNA synthesis. *Annu Rev Biochem* 57:349–374.
89. Kunkel TA (1992) DNA replication fidelity. *J Biol Chem* 267:18251–18254.
90. Trudel M, Van Genechten T, Meuth M (1984) Biochemical characterization of the hamster thy mutator gene and its revertants. *J Biol Chem* 259:2355–2359.
91. Weinberg GL, Ullman B, Wright CM, Martin DW, Jr (1985) The effects of exogenous thymidine on endogenous deoxynucleotides and mutagenesis in mammalian cells. *Somat Cell Mol Genet* 11:413–419.
92. Sánchez A, et al. (2012) Replication fork collapse and genome instability in a deoxycytidylate deaminase mutant. *Mol Cell Biol* 32:4445–4454.
93. Amin NS, Nguyen MN, Oh S, Kolodner RD (2001) exo1-dependent mutator mutations: Model system for studying functional interactions in mismatch repair. *Mol Cell Biol* 21:5142–5155.
94. Janke C, et al. (2004) A versatile toolbox for PCR-based tagging of yeast genes: New fluorescent proteins, more markers and promoter substitution cassettes. *Yeast* 21:947–962.
95. Käufer NF, Fried HM, Schwindinger WF, Jasin M, Warner JR (1983) Cycloheximide resistance in yeast: The gene and its protein. *Nucleic Acids Res* 11:3123–3135.
96. Li L, Murphy KM, Kanevets U, Reha-Krantz LJ (2005) Sensitivity to phosphonoacetic acid: A new phenotype to probe DNA polymerase delta in *Saccharomyces cerevisiae*. *Genetics* 170:569–580.
97. Putnam CD, Hayes TK, Kolodner RD (2009) Specific pathways prevent duplication-mediated genome rearrangements. *Nature* 460:984–989.
98. Sikorski RS, Hieter P (1989) A system of shuttle vectors and yeast host strains designed for efficient manipulation of DNA in *Saccharomyces cerevisiae*. *Genetics* 122:19–27.